The $^2\Pi \leftarrow X\ ^2\Pi$ electronic spectra of C_8H and $C_{10}H$ in the gas phase

Harold Linnartz, Tomasz Motylewski, and John P. Maier
Institute for Physical Chemistry, University of Basel, Klingelbergstrasse 80, CH 4056 Basel, Switzerland

(Received 30 April 1998; accepted 3 June 1998)

The $^2\Pi \leftarrow X\ ^2\Pi$ electronic transition of linear C_8H/C_8D and $C_{10}H/C_{10}D$ has been detected in the gas phase. The carbon radical chains were produced at low temperatures in a pulsed slit nozzle, incorporating a discharge in a high pressure expansion. Cavity ring down spectroscopy is used as a sensitive technique to observe the band systems in absorption. The 0_0^0 band of the $^2\Pi_{3/2} \leftarrow X\ ^2\Pi_{3/2}$ electronic transition of C_8H in the gas phase has its origin near 15 973.5 cm^{-1}, whereas that of $C_{10}H$ is around 14 000 cm^{-1}. Some transitions involving vibrational excitation in the upper $^2\Pi$ electronic state have been also detected. These measurements were undertaken because carbon chains are among the appealing candidates as carriers of diffuse interstellar bands; the observed origin bands do not show matches with the hitherto reported wavelengths. However, these gas phase data now provide a firm basis for a specific astronomical search. © *1998 American Institute of Physics.* [S0021-9606(98)00934-9]

I. INTRODUCTION

It has long been the aim to obtain gas phase electronic spectra of carbon chains. First results were obtained for the anions C_{2n+1}^- ($n=2-5$) using resonance enhanced multiphoton electron detachment, though the bands were all broad.[1,2] A systematic search in the gas phase became possible after the electronic transitions of several carbon chains were identified in 5 K neon matrices.[3] On the basis of these data the electronic spectra of carbon chain anions C_n^- ($n=4,6-8,10$) (Refs. 4–6) and $C_{14}H^-$ (Ref. 7) could be detected in the gas phase. Similarly, guided by the observation in a neon matrix the $^2\Pi \leftarrow X\ ^2\Pi$ band system of the linear carbon radical C_6H was detected by cavity ringdown spectroscopy in a discharge cell[8] and subsequently, rotationally resolved, in a supersonic jet.[7] It has now proven possible to observe the origin bands of the $^2\Pi \leftarrow X\ ^2\Pi$ electronic transitions of C_8H and $C_{10}H$ in the gas phase.

These spectra are especially of interest from an astrophysical point of view. It is argued that carbon chains may play a role as possible carriers of some of the diffuse interstellar bands.[9,10] The first experimental indication of this came from observations of the electronic absorption spectra of mass-selected carbon species in neon matrices.[11] Coincidences between laboratory data and diffuse interstellar band wavelengths have recently been found for vibrational bands in the $A\ ^2\Pi_u \leftarrow X\ ^2\Pi_g$ electronic transition of C_7^- in the gas phase.[7] Following the laboratory detection of the rotational spectra of long cyano-polyacetylenes and highly unsaturated carbon chains in their ground states by microwave spectroscopy,[12] several carbon species, including C_8H, have been identified by radio astronomy in dark interstellar clouds and circumstellar shells.[13] It is expected that long nonpolar pure carbon chains are also present in the interstellar medium and, so far, C_3 and C_5 have been identified near carbon rich stars.[14] In the laboratory, rotationally resolved infrared spectra of linear carbon chains C_n ($n=4-7,9,11,13$) have been reported.[15,16]

In the present experiment cavity ring down spectroscopy is combined with a supersonic plasma generated in a slit nozzle expansion. Cavity ring down spectroscopy has important advantages compared with conventional absorption techniques. Both the immunity to pulse-to-pulse fluctuations in the laser power and the very long absorption pathlengths that are obtained by confining a light pulse in an optical cavity, make this technique ideal to study molecules that are hard to generate in large abundances. Since its introduction in 1988 (Ref. 17) the technique has been applied in many different fields, varying from trace gas detection and combustion processes to cell discharges and molecular beam expansions.[18] Both pulsed and cw lasers, as well as narrow band and polychromatic light sources have been used successfully, showing the strength of cavity ring down as a spectroscopic technique (see, e.g., Refs. 19–21). The combination with a supersonic slit nozzle discharge is new.

Supersonic slit nozzle expansions are standardly used for the investigation of weakly bound molecular complexes.[22] In recent years much effort has been put in combining this method with plasma techniques.[23] Intense beams of rotationally cold radicals,[23] ions,[24] and ionic complexes[25] have been spectroscopically observed. Here a pulsed source has been used, based on the principle described,[23] but which is substantially modified in order to generate larger carbon species in detectable amounts.

II. EXPERIMENT

The experimental setup consists of a standard cavity ring down unit sampling the plasma generated in a pulsed supersonic slit jet expansion. The latter is located in a vacuum chamber that is evacuated by a roots blower system. The orifice of the nozzle comprises a ceramic insulator, metal plate, second insulator, and two sharp stainless steel jaws that form the actual slit (30 mm$\times$300 μm). A pulsed valve with a 2 mm diam orifice is mounted on top of the body and controls the gas flow into the system. Typically, gas mixtures

of 0.2% C_2H_2 or C_2D_2 in Ar with backing pressures of 11 bar are used. A pulsed negative voltage (150 μs, -800 to -1200 V) is applied to both jaws via two separate 4 kΩ ballast resistors and the discharge strikes to the grounded inner metal plate. The geometry of the orifice is such that the discharge is confined upstream of the supersonic expansion. This results in an efficient cooling as the localized discharge *before* the expansion does not interfere with the subsequent cooling *in* the expansion.

The whole experiment runs at 30 Hz. A master trigger is sent to a delay generator from which the laser, gas valve, and discharge are triggered independently. The signal is displayed on a fast oscilloscope and the ring down times of 45 laser shots are averaged at each wavelength before the digitized data are downloaded to a computer.

III. RESULTS AND DISCUSSION

The $^2\Pi \leftarrow X\ ^2\Pi$ electronic spectra of C_8H and $C_{10}H$ were initially identified in absorption in a 5 K neon matrix using mass selection.[26] Data on isoelectronic species and carbon chains of comparable length, HC_6H^+ (Ref. 27) and C_6H,[8] indicate that the matrix spectra are 120–150 cm^{-1} red-shifted of the gas phase value due to solvation. For C_8H accurate ground state constants are available from microwave work.[28]

A. C_8H and C_8D

1. Origin band

The origin band (0_0^0) of the $^2\Pi \leftarrow X\ ^2\Pi$ electronic transition of C_8H is located at 15 844 cm^{-1} in a neon matrix. Thus it was anticipated that in the gas phase this band will lie between 15 965 and 15 995 cm^{-1}. Indeed absorption signals were found in this region. Spectra shown in Fig. 1 were obtained in acetylene or dideuteroacetelyne-argon plasmas. The spectrum recorded with the C_2H_2/Ar mixture shows a strong feature centered around 15 973.5 cm^{-1} that exhibits a double band structure resembling an unresolved P and R branch structure and a weak feature at 15 991 cm^{-1}. The blue shift of the strong band relative to the neon matrix value is roughly 130 cm^{-1}, which is comparable to the 143 cm^{-1} shift found for the $^2\Pi \leftarrow X\ ^2\Pi$ transition of the isoelectronic HC_8H^+.[3] The strong and weak bands shift in the gas phase by 30.5 and 29.3 cm^{-1} to the blue [Fig. 1(c)] upon going from C_8H to C_8D, which matches the shift of 29 ± 5 cm^{-1} found in the neon matrix experiment.[29] The uncertainty in the matrix data, which can become as large as 10 cm^{-1}, is due to the broadness of the bands.

The structural parameters of C_8H in its ground electronic state are known from microwave spectroscopy.[28] As for all the C_nH species with $n>4$ the ground state of C_8H has $^2\Pi$ symmetry. For the even species, $C_{2n}H$, this state is inverted, i.e., the $\Omega=\frac{3}{2}$ spin–orbit component lies lower in energy than $\Omega=\frac{1}{2}$. One expects to observe two components in the electronic spectrum, separated by the difference of the spin–orbit constants $|A'-A''|$, consisting of P, R and a weak Q branch, as it was observed for C_6H.[7] The relative intensity of the spin–orbit components is strongly influenced by the value of A'', because of the low rotational temperatures in the jet, approximately 10–50 K.

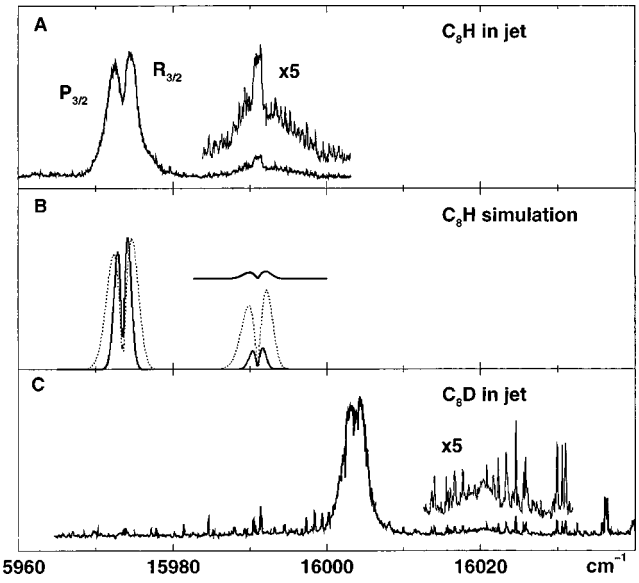

FIG. 1. Origin band of the $^2\Pi \leftarrow X\ ^2\Pi$ electronic transition of C_8H (a) and C_8D (c), observed by cavity ring down spectroscopy in a pulsed slit jet plasma. The different intensity ratio of the C_8H and C_8D bands relative to the sharp absorption lines (which originate most likely from C_2) are due to different expansion conditions. (b) shows a simulation of the C_8H spectrum for $T_{rot}=15$ K (bold line) and $T_{rot}=50$ K (dotted line), using for the ground state the constants determined by microwave spectroscopy (Ref. 28) and $A'=-36.8$ cm^{-1}. The inset shows the simulation for $T_{rot}=50$ K, assuming the band near 15 991 cm^{-1} to be a sequence transition of the lowest frequency bending mode.

In case of C_6H both $^2\Pi_{1/2} \leftarrow X\ ^2\Pi_{1/2}$ and $^2\Pi_{3/2} \leftarrow X\ ^2\Pi_{3/2}$ band systems were observed, though the former one is weaker.[7] The analysis of the rotationally resolved spectrum showed that $A'>A''$. For C_8H only one band is clearly visible, the second one being relatively weak [inset of Fig. 1(a)]. The latter shows a strange pattern which is caused by the overlap of absorption lines of a pure carbon species, most likely C_2, as can be concluded from the spectrum obtained in the C_2D_2/Ar plasma. The corresponding band for C_8D, partially covered with other lines as well, is shown in the inset of Fig. 1(c). It appears logical at a first view to assign the strong band to the $\Omega=\frac{3}{2}$ and the weak one to the $\Omega=\frac{1}{2}$ component in analogy to C_6H. A ''spin–orbit temperature'' of about 15 K in the plasma is estimated from the relative intensities of the components, using $A''=-19.33$ cm^{-1}.[28] It is expected that in supersonic rare gas expansions the spin–orbit and rotational cooling is comparable.[30]

Although spectroscopy in slit nozzle expansions is nearly Doppler free, rotational structure is not resolved in the C_8H spectrum due to the bandwidth of the laser (0.15 cm^{-1}). Therefore, the rotational profile was simulated [Fig. 1(b), bold line]. The constants determined by microwave spectroscopy for the $X\ ^2\Pi$ ground state were used. The calculated profile was compared to the observed spectrum, with B', A', and $\nu_{00}(\Omega=\frac{3}{2})$ as parameters. The temperature was kept fixed to the derived 15 K, assuming an efficient spin–orbit

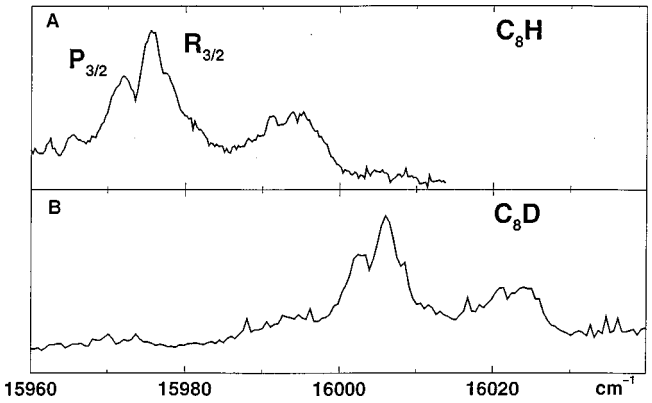

FIG. 2. Origin band of the $^2\Pi \leftarrow X\ ^2\Pi$ electronic transition of C_8H (top trace) and C_8D (bottom trace), detected by cavity ring down spectroscopy in a liquid nitrogen cooled hollow cathode discharge cell ($T_{rot} \approx 150$ K).

cooling to take place. The separation and relative intensities are best fitted with $\nu_{00} = 15\,973.5(2)$ cm^{-1}, $A' = -36.8(2)$ cm^{-1}, and B' within 1% of the B'' value. However, the band shape is not reproduced correctly. As can be seen from comparing Figs. 1(a) and 1(b) the rotational contour is considerably narrower in the simulation than in the observed spectrum. This may be explained by the effect that in jet expansions higher rotational levels cool less efficiently than the lower ones, yielding different temperature regimes for the rotational levels.[31] However, the rotational profile of the strong band is better simulated with 50 K [dotted line, Fig. 1(b)]; both the line shapes and the Boltzmann maxima are in much better agreement, but now the relative intensity of the spin–orbit components is wrong.

In order to have an additional check on the behavior of the weak component a spectrum was recorded in a pulsed hollow cathode discharge cell cooled by liquid nitrogen. In such a setup rotational temperatures around 150 K were inferred from the electronic spectrum of C_6H.[8] The present spectra recorded with mixtures of 1% C_2H_2 and C_2D_2 in He (600 V, 1.5 A, 60 μs pulses) are shown in Figs. 2(a) and 2(b). Some weaker bands arise from other carbon species, because no significant shift is observed upon deuteration. The two main features seen in the slit jet are present, as well as additional bands, caused by the higher rotational, vibrational and translational temperatures that are typical for discharge cells. Under these conditions the spectrum can become congested by vibrational hot and sequence bands, as was the case for C_6H.[8] The effect of less efficient cooling in the cell is also visible from the shift of the Boltzmann distribution to higher J-values. The band around 15 991 cm^{-1} is now stronger [Fig. 2(a)], but at $T_{rot} = 150$ K nearly equal intensities are expected for the two spin–orbit components.

Unless the spin–orbit and rotational temperature are quite different, then the jet and cell observations suggest a different assignment of the 15 991 cm^{-1} band, i.e., to sequence transition(s). Seven degenerate bending modes of C_8H have been calculated to lie in the 60–600 cm^{-1} range.[32] The lowest frequency bending mode near 62 cm^{-1} has a population of about 15% relative to the $\nu = 0$ level for temperatures of 50 K and 55% at 150 K, which is close to the observed band intensity ratios. At 150 K the other low lying bending modes can reach populations up to 20%, which may explain some of the additional bands observed in Fig. 3. This analysis implies that the second spin–orbit component is hidden under the strong band, yielding $|A' - A''| < 1.5$ cm^{-1}, because for larger differences the asymmetry in the $^2\Pi_{3/2} \leftarrow X\ ^2\Pi_{3/2}$ band should have been observed. The weak band near 15 991 cm^{-1} could then be a sequence transition of the ≈ 62 cm^{-1} bending mode. This gives a reasonable intensity ratio as shown in the simulation [inset of Fig. 1(b)]. However, at this stage it is not possible to locate unambiguously the origin band of the $\Omega = \frac{1}{2}$ component.

2. 3_0^1 and 5_0^1 bands

In the C_8H absorption spectrum recorded in the neon matrix, transitions to several vibrationally excited levels in the upper $^2\Pi$ electronic state have been detected.[26] The single excitation of the ν_3 and ν_5 totally symmetric stretch-

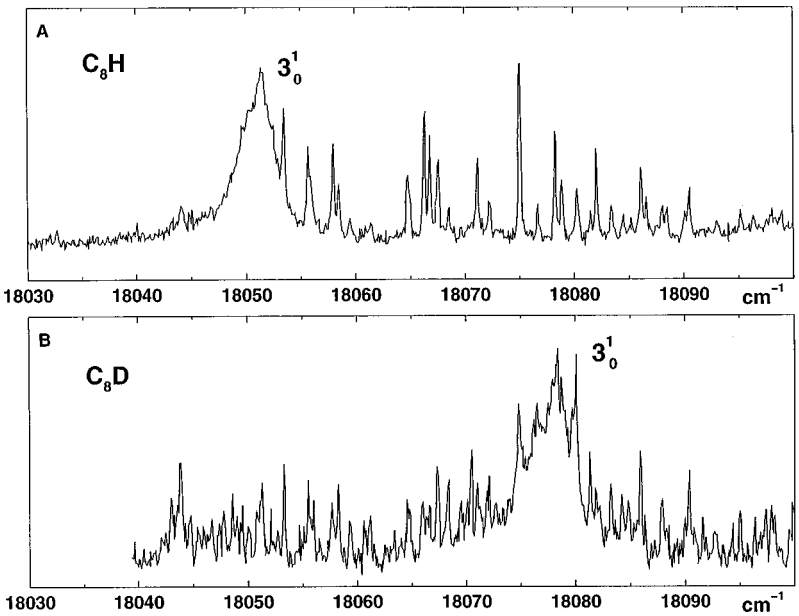

FIG. 3. Vibronic band involving the ν_3 totally symmetric stretching mode in the $^2\Pi \leftarrow X\ ^2\Pi$ electronic transition of C_8H (top trace) and C_8D (bottom trace). The sharp lines arise from the C_2 $d\ ^3\Pi_g \leftarrow a\ ^3\Pi_u$ Swan system and vary in intensity in both figures due to different expansion conditions.

TABLE I. Gas phase data on the $^2\Pi \leftarrow X\ ^2\Pi$ electronic transition of C_8H/C_8D. The estimated band origin is given for the 0_0^0 transition, whereas for the other vibrational bands the maximum of the contour is listed. The values observed in a neon matrix are given for comparison. All frequencies are in vacuum wave numbers.

$^2\Pi \leftarrow X\ ^2\Pi$			Gas phase			Neon matrix			$\nu_{gas} - \nu_{matrix}$
		Ω	ν	Interval	$C_nH \rightarrow C_nD$	ν	Interval	$C_nH \rightarrow C_nD$	($\pm 5\ cm^{-1}$)
C_8H	0_0^0	$\frac{3}{2}$	15 973.5(2)	0		15 844(5)[a]	0		130
	3_0^1		18 051.1(5)	2077.6		17 914(5)[b]	2070		137
	5_1^0		17 564.7(5)	1591.2		17 450(5)[a]	1606		115
C_8D	0_0^0	$\frac{3}{2}$	16 004.0(3)	0	30.5	15 873(5)[c]	0	29	131
	3_0^1		18 077.8(5)	2073.8	26.7	17 937(5)[c]	2064	23	141
	5_0^1		17 596.3(3)	1592.3	31.6	17 477(5)[c]	1604	27	119

[a]Reference 26.
[b]Reanalyzed data from Ref. 26.
[c]Reference 29.

ing modes—3_0^1 and 5_0^1—have been located at 2070 and 1606 cm^{-1} to higher energy of the $\Omega = \frac{3}{2}$ origin band. The maximum of these bands is found in the gas phase around 18 051 and 17 565 cm^{-1}, which corresponds to vibrational frequencies of ≈2078 and 1591 cm^{-1}, respectively. The 3_0^1 and 5_0^1 bands of C_8D have been observed as well. The shifts going from C_8H to C_8D in the gas phase match well the matrix data.[29] In Fig. 3 the 3_0^1 band of the $^2\Pi \leftarrow X\ ^2\Pi$ electronic transition of C_8H and C_8D is shown. Other bands that were found in the solid neon environment are below the detection limit of the cavity ring down setup. The observed gas phase transitions are listed in Table I.

B. $C_{10}H$ and $C_{10}D$: Origin and 3_0^1 band

The 0_0^0 band of the $^2\Pi \leftarrow X\ ^2\Pi$ electronic transition of $C_{10}H$ has been observed in a neon matrix at 13 848 cm^{-1}.[26] In the slit jet experiment the origin band has its maximum at 14 000 cm^{-1} for $C_{10}H$ and at 14 020 cm^{-1} for $C_{10}D$ (Fig. 4), shifted by approximately 150 cm^{-1} to the blue of the neon matrix values (Table II). The isotopic shift going from $C_{10}H$ to $C_{10}D$ is 20 cm^{-1}, close to the (18 ± 4) cm^{-1} shift found in a 5 K neon matrix.[29] The observed band is assumed to be of the $\Omega = \frac{3}{2}$ component. The width of the band is approximately 5 cm^{-1} which is slightly larger than for C_8H. Up to now no microwave constants of $C_{10}H$ have been published. A simulation of the rotational band profile, in view of the poor signal to noise ratio and anticipated presence of overlapping vibrational sequences, was not possible.

The 3_0^1 transition in the $^2\Pi \leftarrow X\ ^2\Pi$ band system has been located in the neon matrix at 15 945 cm^{-1} for $C_{10}H$ and at 15 960 cm^{-1} for $C_{10}D$.[26,29] Transitions to other vibrationally excited levels in the upper electronic $^2\Pi$ state only show moderate intensity. In the gas phase spectrum, the maximum of the 3_0^1 band of $C_{10}D$ is found around 16 102 cm^{-1}. The corresponding spectrum of $C_{10}H$ shows two bands, one around 16 075 cm^{-1}, the other around 16 084 cm^{-1}. Comparing gas and neon frequency values, suggests that the latter one is more likely to be the 3_0^1 transition.

IV. ASTROPHYSICAL CONSEQUENCES

As was concluded earlier for C_6H,[8] also in the case of the $^2\Pi \leftarrow X\ ^2\Pi$ transition of C_8H and $C_{10}H$, the $\Omega = \frac{3}{2}$ origin bands do not coincide with wavelengths of published diffuse interstellar bands.[33] The 0_0^0 band ($\Omega = \frac{3}{2}$) of C_8H is far away from any listed DIB. The origin band of $C_{10}H$ is close to a broad DIB positioned at 14 005.7 cm^{-1} and the 3_0^1 transition matches a DIB listed as probable at 16 083.8 cm^{-1}. The latter two DIBs, however, have quite different half-widths and equivalent strengths, which makes it unlikely that they originate from the same carrier. Nevertheless, the availability of the gas phase data open the way to specific astronomical searches.

ACKNOWLEDGMENT

This research has been supported by the Swiss National Science Foundation, Project No. 20-29104.96.

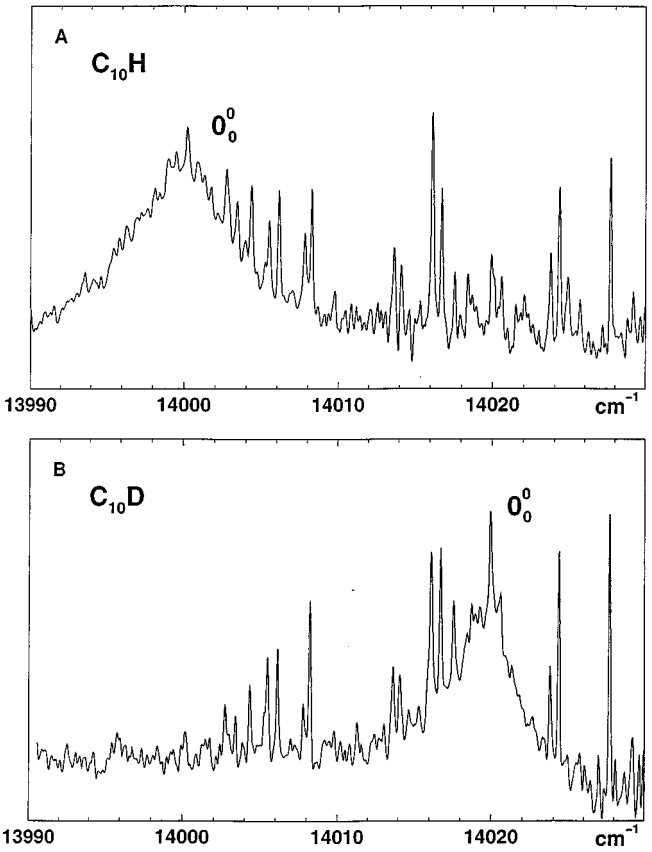

FIG. 4. Origin band of the $^2\Pi \leftarrow X\ ^2\Pi$ electronic transition of $C_{10}H$ (top trace) and $C_{10}D$ (bottom trace).

TABLE II. Gas phase data on the $^2\Pi \leftarrow X\ ^2\Pi$ electronic transition of $C_{10}H/C_{10}D$ (maximum of bands) and those in a neon matrix. All frequencies are in vacuum wave numbers.

$^2\Pi \leftarrow X\ ^2\Pi$			Gas phase			Neon matrix			$\nu_{gas} - \nu_{matrix}$
		Ω	ν	Interval	$C_nH \rightarrow C_nD$	ν	Interval	$C_nH \rightarrow C_nD$	(± 5 cm^{-1})
$C_{10}H$	0_0^0	$\frac{3}{2}$	14 000(1)	0		13 848(4)[a]	0		152
	3_0^1		16 084(2)	2084		15 945(4)[a]	2097		139
			16 075(2)	2075					130
$C_{10}D$	0_0^0	$\frac{3}{2}$	14 020(1)	0	20	13 866(4)[b]	0	18	154
	3_0^1		16 102(1)	2082	18–27	15 960(4)[b]	2094	15	142

[a]Reference 26.
[b]Reference 29.

[1] M. Ohara, H. Shiromaru, Y. Achiba, K. Aoki, K. Hashimoto, and S. Ikuta, J. Chem. Phys. **103**, 10393 (1995).
[2] M. Ohara, H. Shiromaru, and Y. Achiba, J. Chem. Phys. **106**, 9992 (1997).
[3] J. P. Maier, Chem. Soc. Rev. **26**, 21 (1997).
[4] Y. Zhao, E. de Beer, and D. M. Neumark, J. Chem. Phys. **105**, 2575 (1996).
[5] Y. Zhao, E. de Beer, C. Xu, T. Taylor, and D. M. Neumark, J. Chem. Phys. **105**, 4905 (1996).
[6] M. Tulej, D. A. Kirkwood, G. Maccaferri, O. Dopfer, and J. P. Maier, Chem. Phys. **128**, 239 (1998).
[7] D. A. Kirkwood, H. Linnartz, M. Grutter, O. Dopfer, T. Motylewski, M. Pachkov, M. Tulej, M. Wyss, and J. P. Maier, Faraday Discuss. (in press).
[8] M. Kotterer and J. P. Maier, Chem. Phys. Lett. **266**, 342 (1997).
[9] A. E. Douglas, Nature (London) **269**, 130 (1977).
[10] *The Diffuse Interstellar Bands*, edited by A. G. G. M. Tielens and T. P. Snow (Kluwer Academic, Dordrecht, 1995).
[11] J. Fulara, D. Lessen, P. Freivogel, and J. P. Maier, Nature (London) **366**, 439 (1993).
[12] M. C. McCarthy, M. J. Travers, A. Kovács, C. A. Gottlieb, and P. Thaddeus, Astrophys. J., Suppl. Ser. **113**, 105 (1997).
[13] J. Cernicharo and M. Guélin, Astron. Astrophys. **309**, L27 (1996).
[14] K. H. Hinkle, J. J. Keady, and P. F. Bernath, Science **241**, 1319 (1988); P. F. Bernath, K. H. Hinkle, and J. J. Keady, *ibid.* **244**, 562 (1989).
[15] J. R. Heath and R. J. Saykally, in *On Clusters and Clustering, From Atoms to Fractals* (Elsevier, New York, 1993), p. 7.
[16] T. F. Giesen, A. van Orden, H. J. Hwang, R. S. Fellers, R. A. Provencal, and R. J. Saykally, Science **265**, 756 (1994).
[17] A. O'Keefe and D. A. G. Deacon, Rev. Sci. Instrum. **59**, 2544 (1988).
[18] M. D. Wheeler, S. M. Newman, A. J. Orr-Ewing, and N. R. Ashfold, J. Chem. Soc., Faraday Trans. **94**, 337 (1998), and references therein.
[19] R. Engeln and G. Meijer, Rev. Sci. Instrum. **67**, 2708 (1996).
[20] D. Romanini, A. A. Kachanov, N. Sadeghi, and F. Stoeckel, Chem. Phys. Lett. **264**, 316 (1997).
[21] R. Engeln, G. Berden, E. van den Berg, and G. Meijer, J. Chem. Phys. **107**, 4458 (1997).
[22] D. J. Nesbitt, Annu. Rev. Phys. Chem. **45**, 367 (1994).
[23] S. Davis, D. T. Anderson, G. Duxbury, and D. J. Nesbitt, J. Chem. Phys. **107**, 5661 (1997), and references therein.
[24] T. Ruchti, T. Speck, J. P. Connelly, E. J. Bieske, H. Linnartz, and J. P. Maier, J. Chem. Phys. **105**, 2591 (1996).
[25] T. Speck, H. Linnartz, and J. P. Maier, J. Chem. Phys. **107**, 8706 (1997); H. Linnartz, T. Speck, and J. P. Maier, Chem. Phys. Lett. **288**, 504 (1998).
[26] P. Freivogel, J. Fulara, M. Jakobi, D. Forney, and J. P. Maier, J. Chem. Phys. **103**, 54 (1995).
[27] D. Klapstein, R. Kuhn, J. P. Maier, M. Ochsner, and W. Zambach, J. Phys. Chem. **88**, 5176 (1984).
[28] J. C. Pearson, C. A. Gottlieb, D. R. Woodward, and P. Thaddeus, Astron. Astrophys. **189**, L13 (1988).
[29] P. Freivogel, Ph.D. thesis, University of Basel, 1997.
[30] P. G. Carrick and P. C. Engelking, Chem. Phys. Lett. **108**, 505 (1984).
[31] T. Speck, H. Linnartz, and J. P. Maier, J. Mol. Spectrosc. **185**, 425 (1997).
[32] O. V. Dorofeeva and L. V. Gurvich, Thermochim. Acta **197**, 53 (1992).
[33] P. Jenniskens and F.-X. Désert, Astron. Astrophys., Suppl. Ser. **106**, 39 (1994).